



University of
Strathclyde
Glasgow

ICF-related research at Strathclyde

Paul McKenna

University of Strathclyde



EPSRC grant: EP/E048668/1

Key physics for ICF diagnosed by ion emission

1. Fast electron generation and transport in dense plasma
2. Shock propagation physics
3. Laser-ion source development (ion fast ignition)
 - (Nuclear diagnostics of laser-plasma)



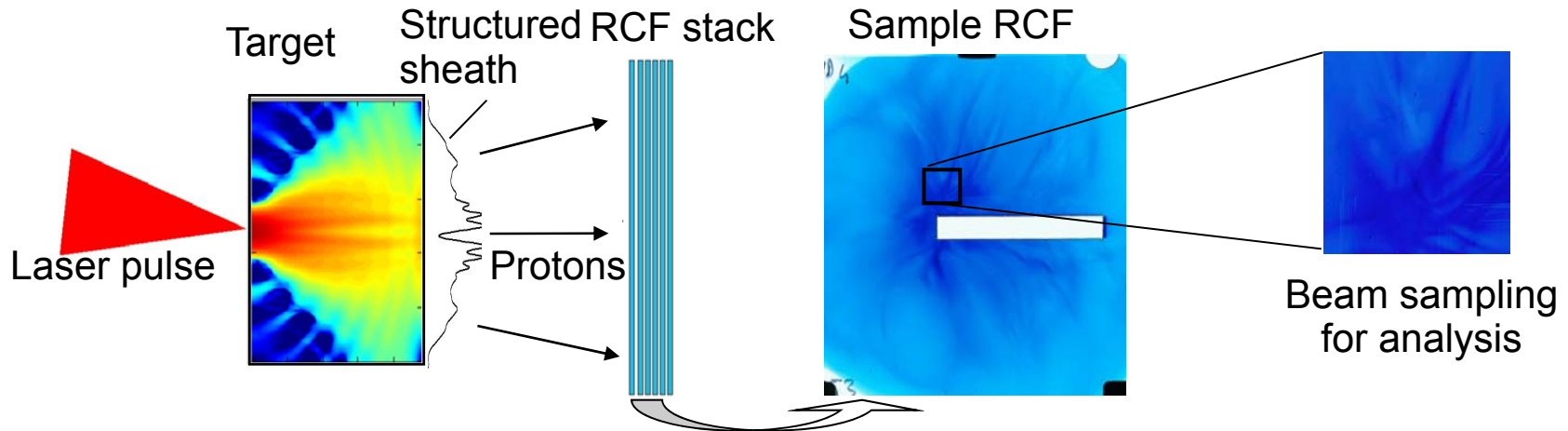
Fast electron generation and transport:

Notoriously difficult to measure fast electrons in solid targets. Each diagnostic has limitations due to assumptions, model dependences etc.

Examples:

<u>Diagnostic</u>	<u>Energy range</u>	<u>Issues</u>
K α emission	10s keV	Wavelength shift with temperature
CTR / OTR emission	MeV	Limited to thin targets due to electron bunch dephasing
“Escaped” electron spectrometry	MeV	Target charges to MV potentials

Our approach: Ion emission as a diagnostic



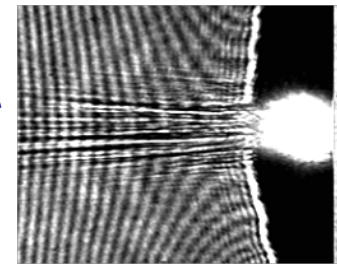
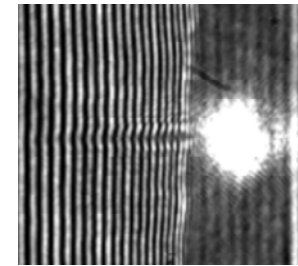
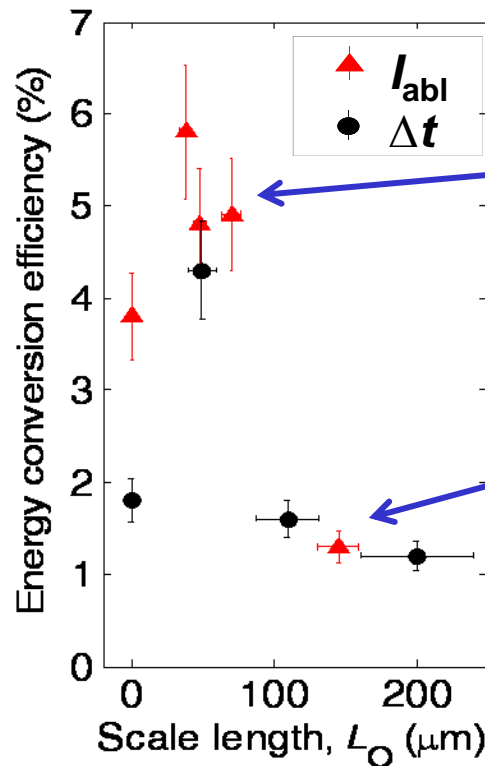
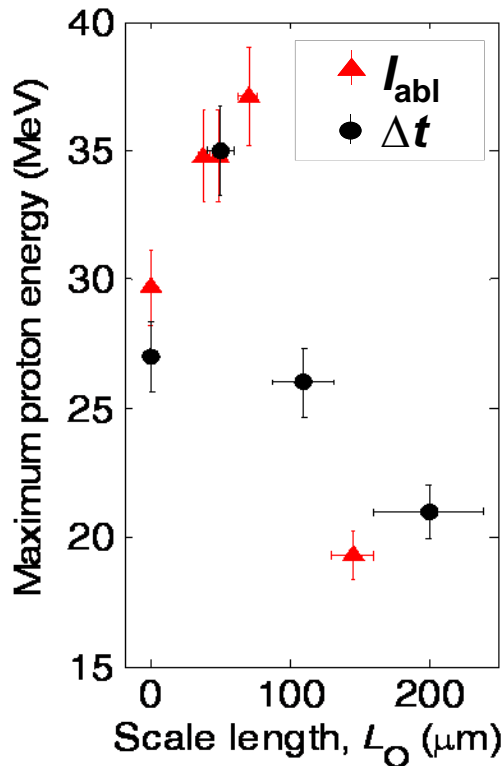
- Maximum proton energy → electron density (MeV energies)
- Intensity distribution → electron transport filamentation
- Proton divergence with energy → electron sheath profile
- Proton spectrum → electron temperature (model)

- Thick solid density targets can be investigated (>mm)

1: Laser propagation and energy absorption

P. McKenna et al, LPB **26** 591-596 (2008)

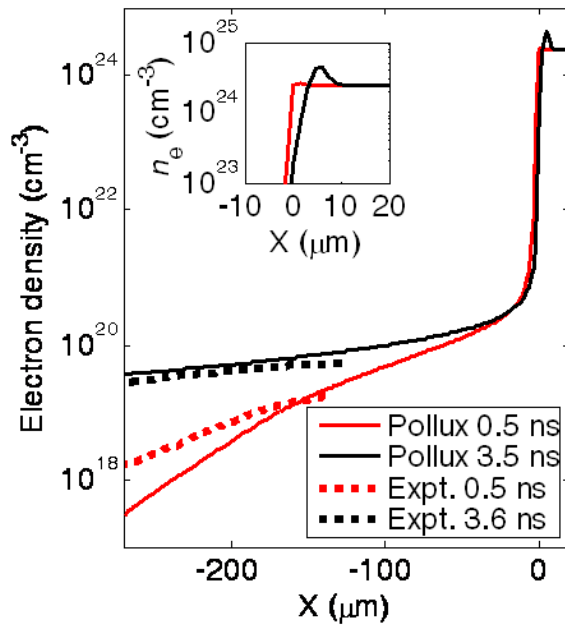
D.C. Carroll et al, CRP **10** 188-196 (2009)



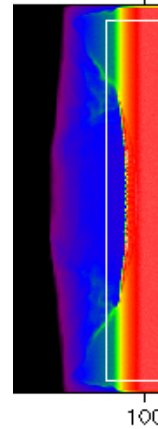
→ Proton measurements show that controlled preplasma expansion leads to enhanced energy coupling to fast electrons

OSIRIS Simulations

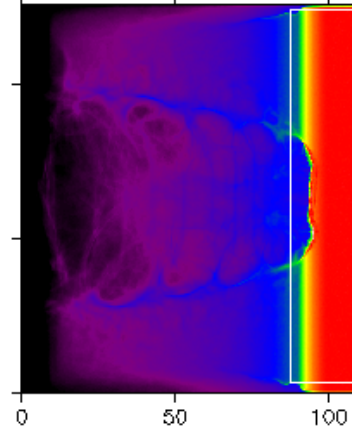
Simulations by Roger Evans



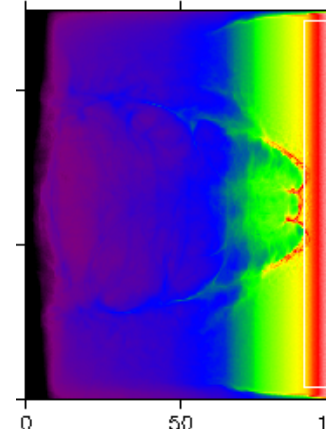
Sharp density gradient



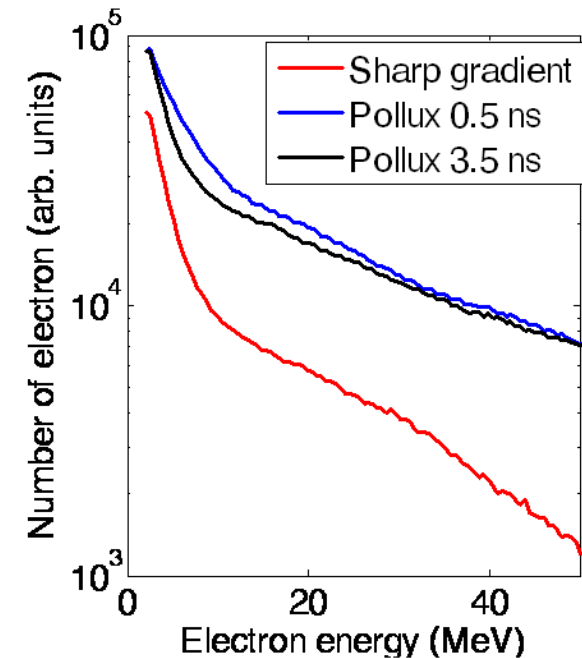
0.5ns Pollux density profile



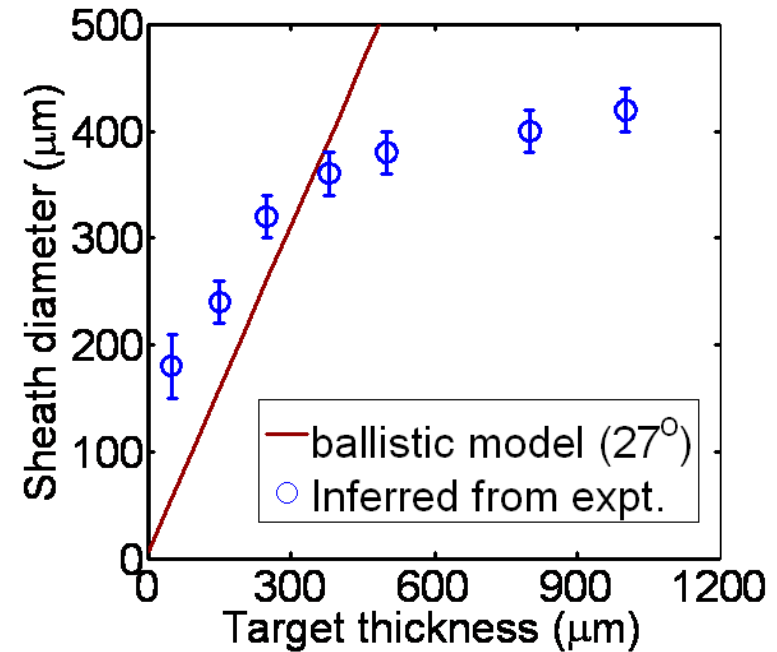
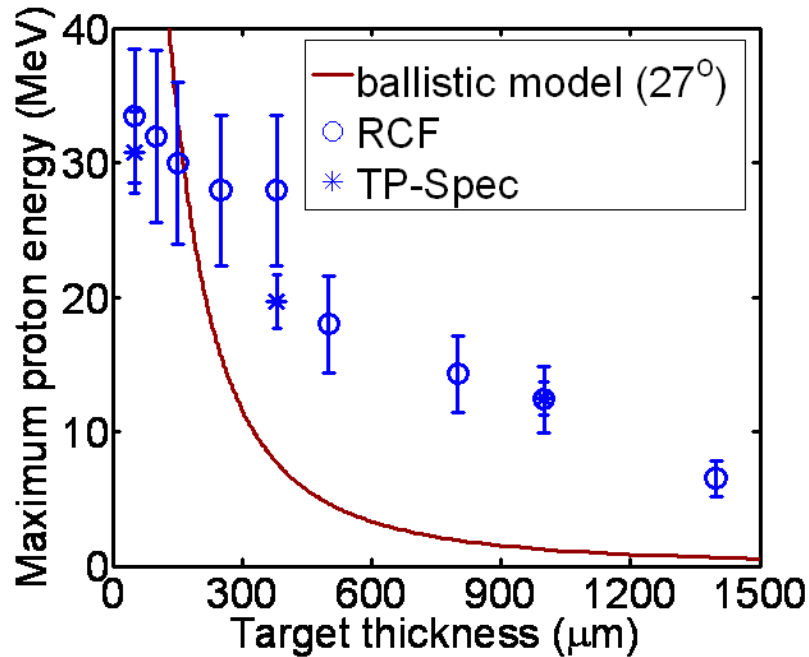
3.5ns Pollux density profile



- Preplasma expansion enhances electron energy spectrum
- Self focusing and beam break-up observed
- changes to the electron injection angle



2. Collimation of fast electron transport

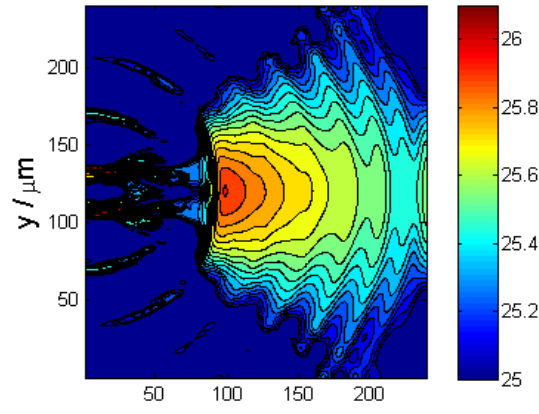


Yuan...McKenna., submitted (2009)

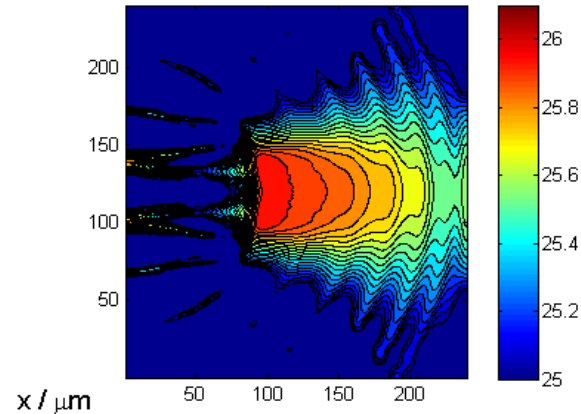
→ Evidence of collimation of fast electrons in solid targets by self-generated B-field observed using proton emission

Simulations with 2-D hybrid LEDA code

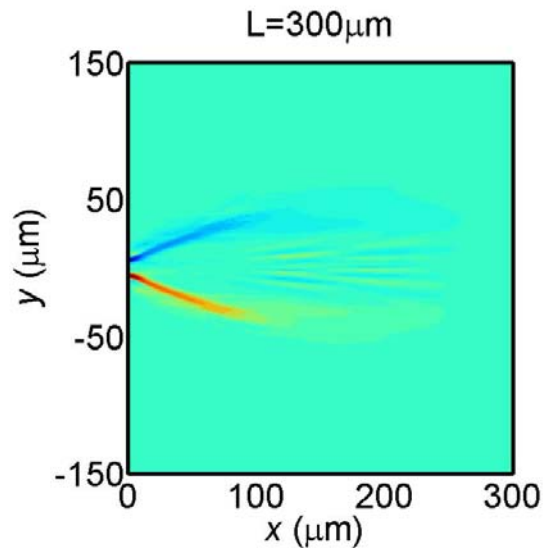
Simulations by Alex Robinson (RAL)



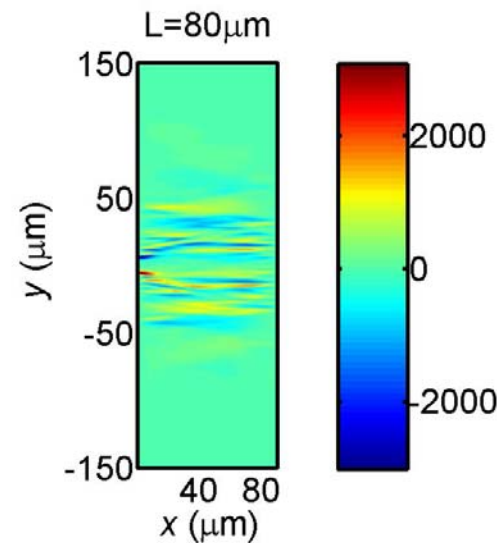
Ne no B field



Ne with B field



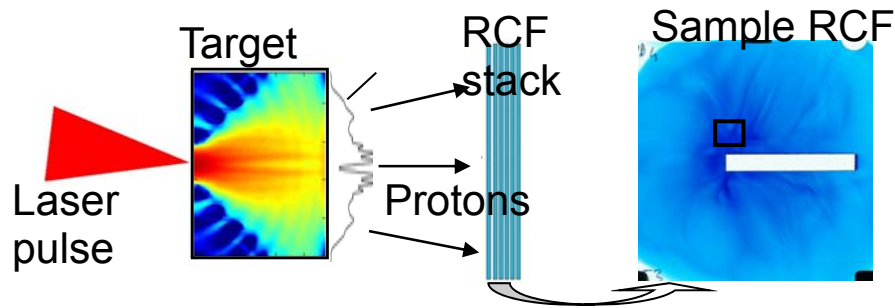
$L=300\mu\text{m}$



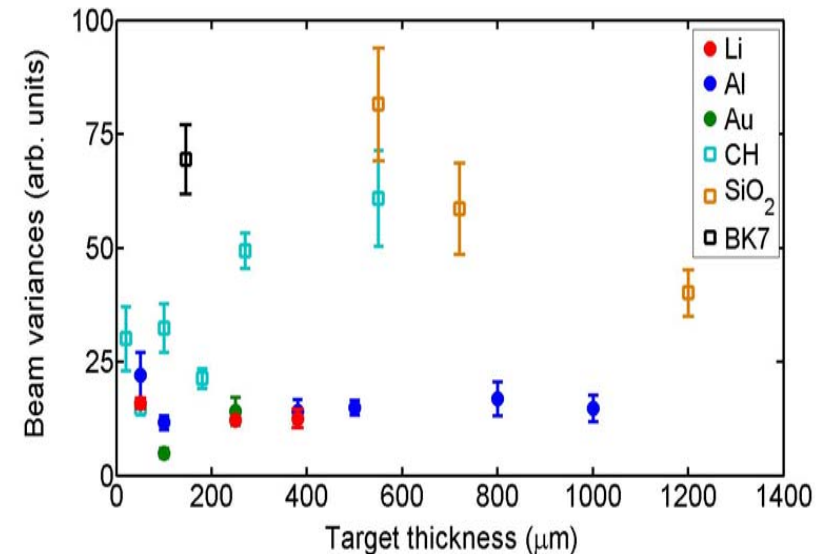
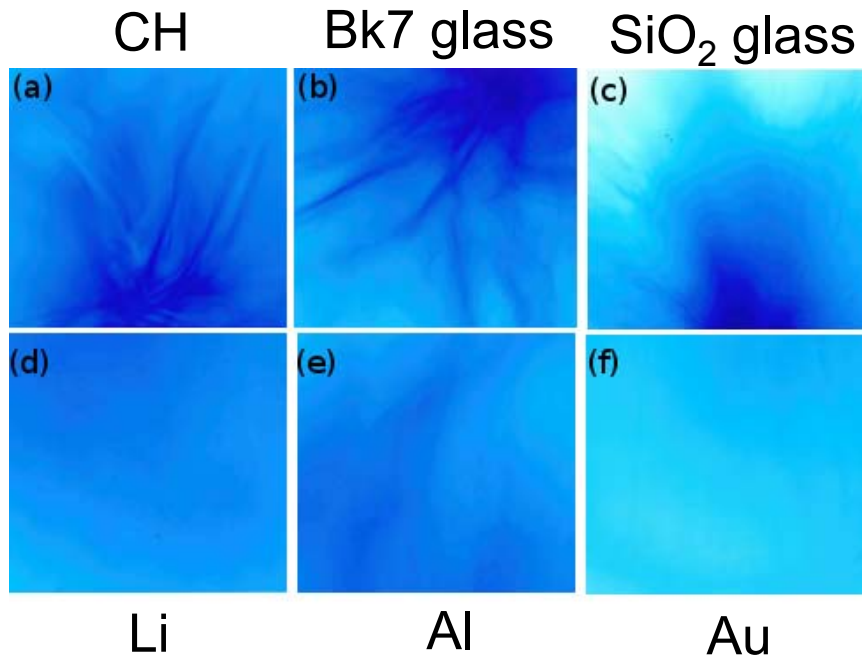
$L=80\mu\text{m}$

Electron refluxing within thin targets perturbs B-field structure

3: Effects of target material on beam filamentation



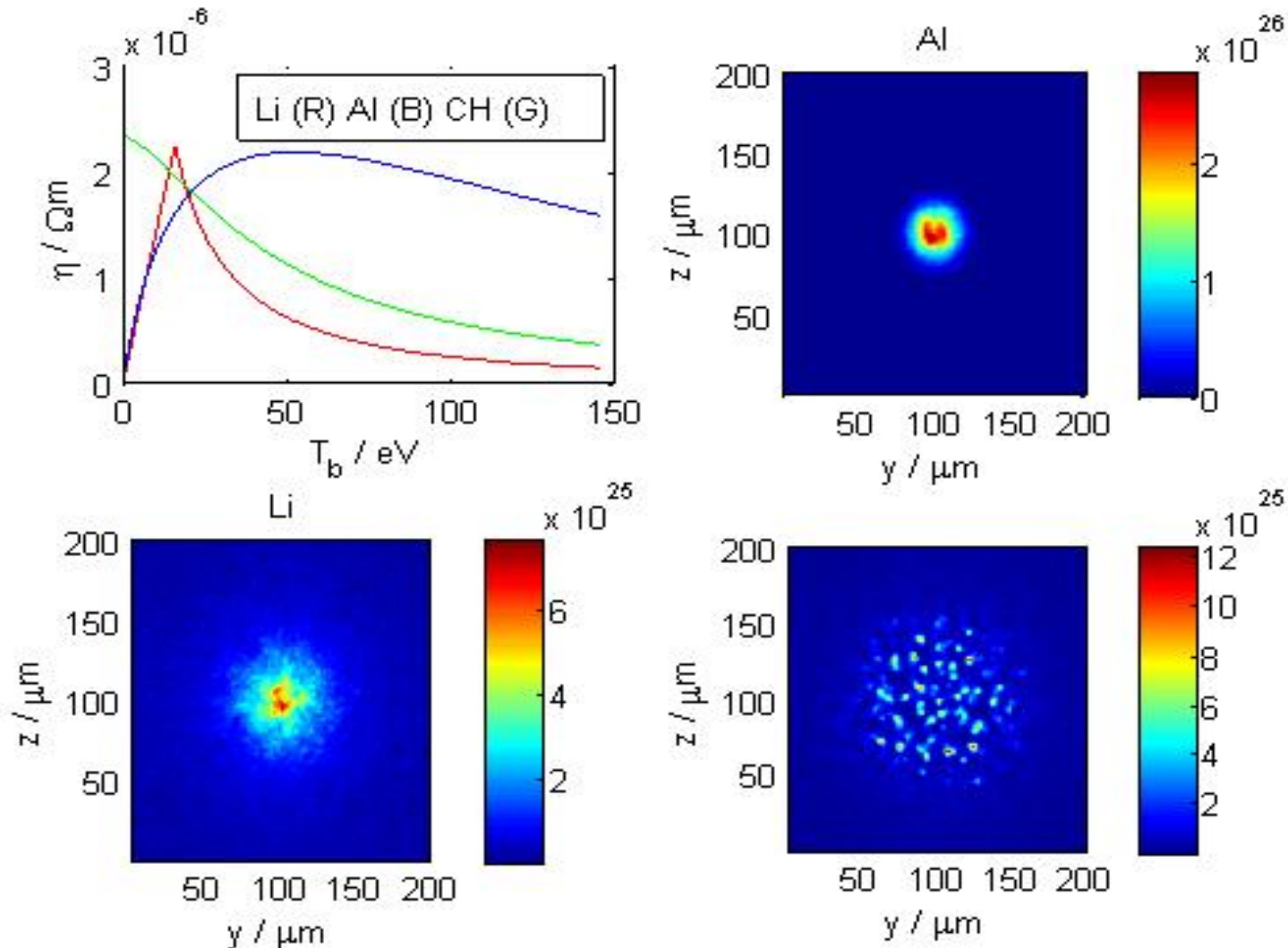
Target	Effective Z	Resistivity [$\Omega \cdot m$]
Al	13	10^{-8}
C_3H_6	5.4	10^{13}
Li	3	10^{-7}
SiO_2	11.6	10^{14}



ZEPHROS hybrid-PIC simulations

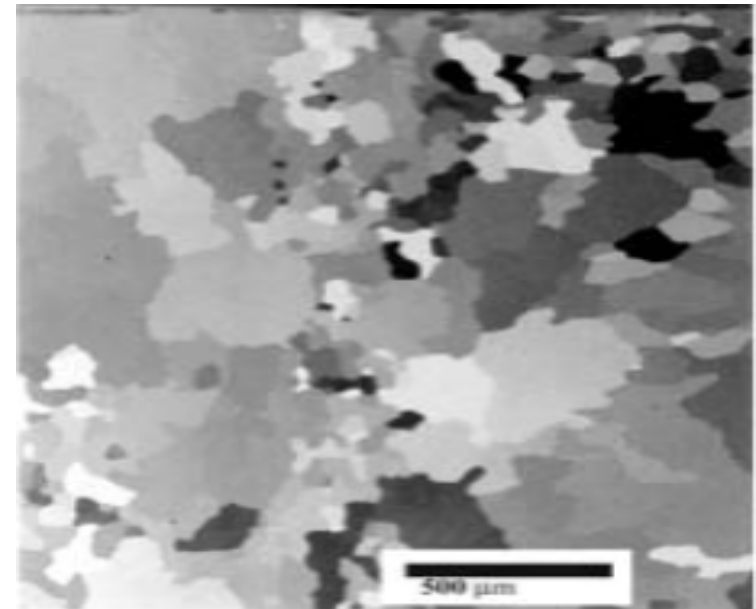
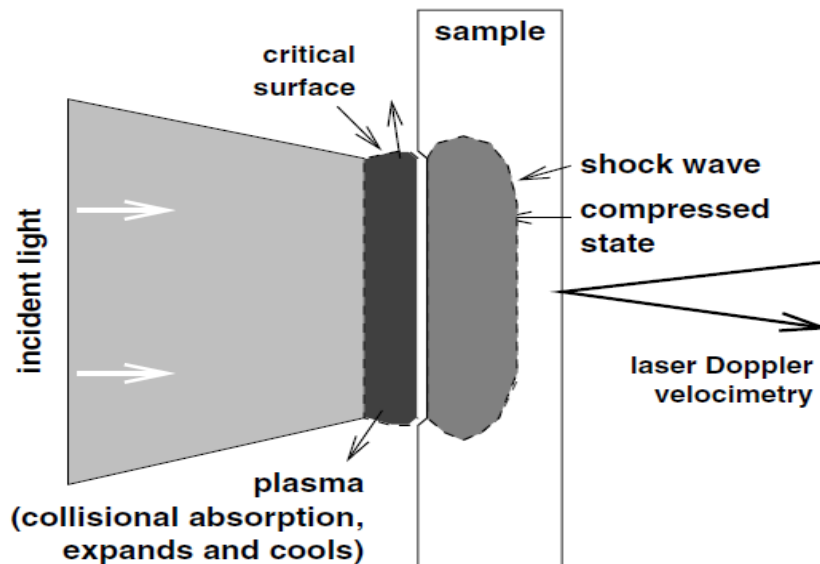
Simulations by Alex Robinson (RAL);

Li curve calculation by Mike Desjarlais (Sandia)



4. Shock propagation physics

- Exception sphericity of implosion required for ICF
- Non-uniformities in illumination or target roughness amplified by Richtmeyer-Meshkov and Rayleigh-Taylor instabilities
- Uniform drive pressure can result in non-uniform shock propagation depending on grain alignment in the material
- e.g. Be is naturally polycrystalline with different shock velocities along different crystal axes – grain size is $\sim 10 \mu\text{m}$

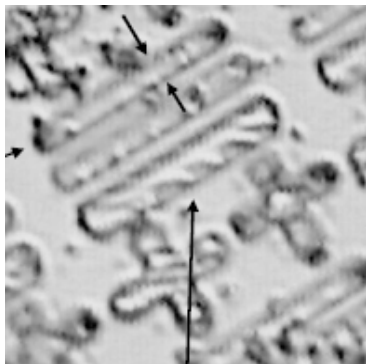


Shock uniformity measurements using proton emission

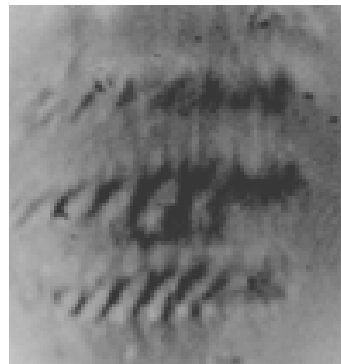
Our approach – use proton emission imaging to measure perturbations of the initial shock breakout

CPA illumination timed to coincide with shock breakout thus imprinting the rear surface geometry on the ion emission.

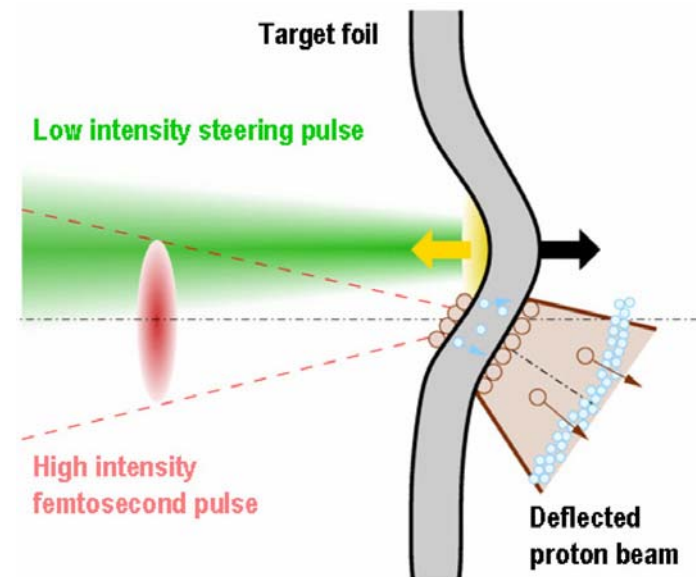
Proof-of-principle tests in January 2010



Sub-micron structure on target surface



Reproduced in proton beam

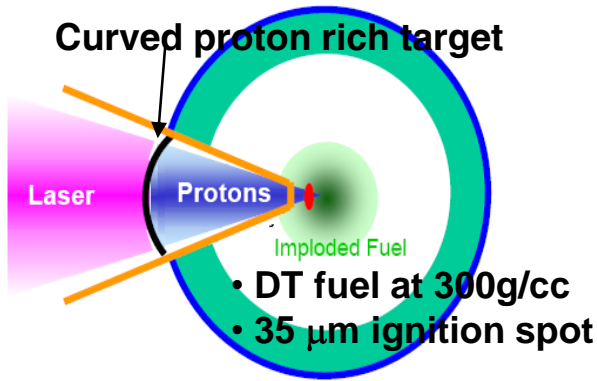


Proton emission is sensitive to shock breakout

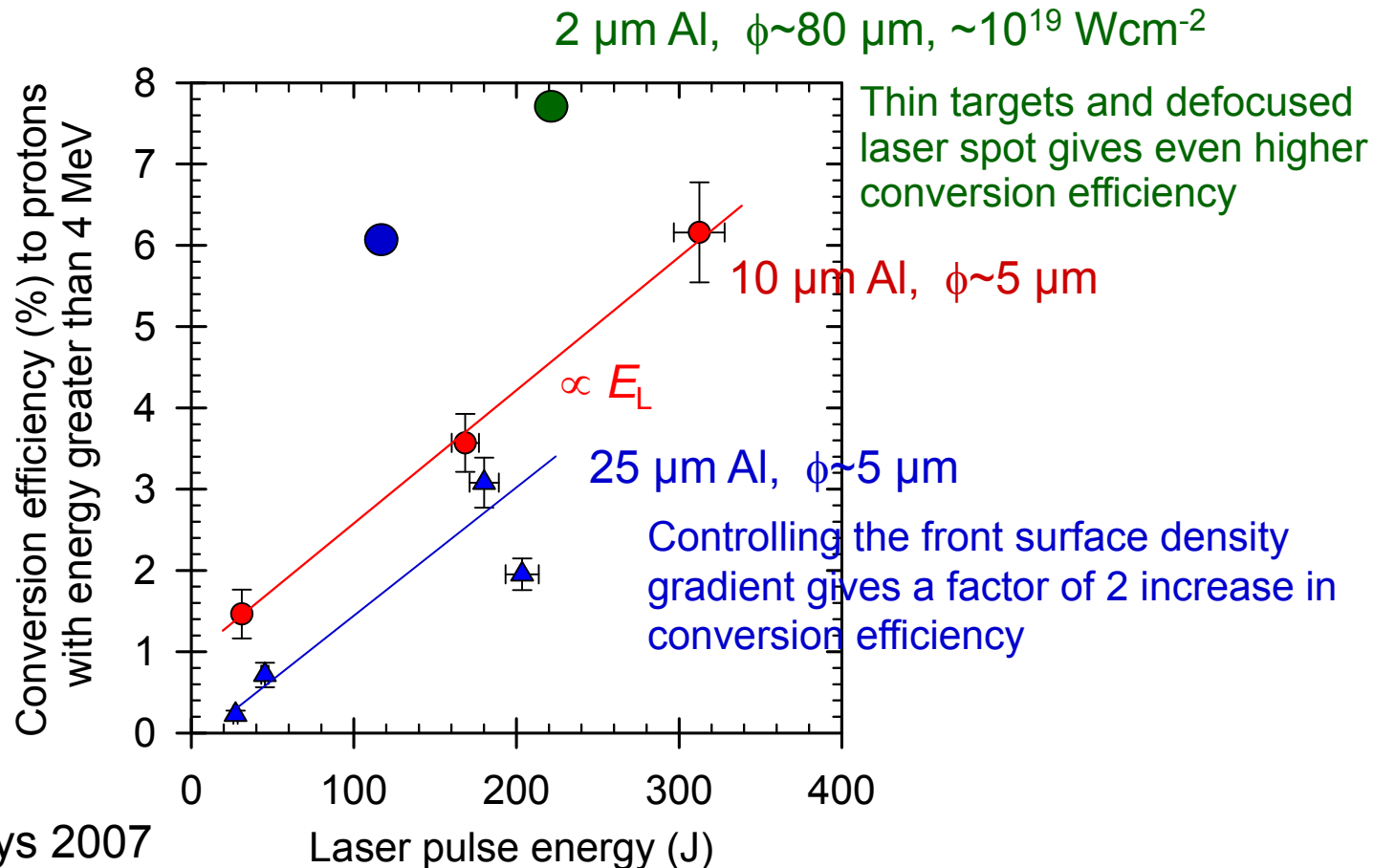
Lindau *et al.*, PRL 95, 175002 (2005)

M. Roth *et al.*, PR-STAB 5, 061301 (2002)

5: Laser-ion source development



- Proton energy scaling with ps pulse
- Spectral shaping with dual CPA pulses
- Techniques to enhance conversion efficiency



Summary of ICF-related physics at Strathclyde

1. Proton emission applied as a diagnostic of fast electron generation and transport

Examples:

- Electron generation as a function of plasma scale length
- Collimating effect of self-generated magnetic fields
- Electron transport filamentation
- Electron transport in compressed targets (HiPER, LULI)

2. Shock propagation physics

- Ion diagnostic technique to be trialled in January 2010

3. Laser-ion source development (ion fast ignition)

- Spectral control and enhancement of conversion efficiency

4. Nuclear diagnostics of laser-plasmas



Collaboration:

P. McKenna et al

SUPA, Department of Physics, University of Strathclyde

D. Neely, A.P.L. Robinson et al

STFC, Rutherford Appleton Laboratory

R G Evans

Imperial College London

M. Borghesi, M. Zepf et al

School of Mathematics and Physics, Queen's University Belfast.

J. Fuchs et al

LULI Ecole Polytechnique, France

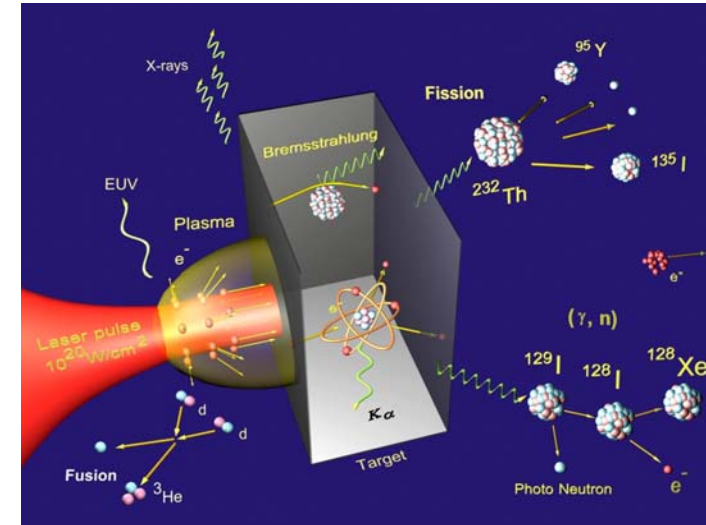
M. P. Desjarlais

Sandia National Laboratories, New Mexico

6: Nuclear activation

1 – Development of laser-plasma nuclear diagnostics

- choice of activation reactions with well-known cross sections;
- spectral, spatial and yield measurements of n , γ , ions;
- significant development work required for in-situ measurements in noisy plasma environment, using radiation hardened detectors;

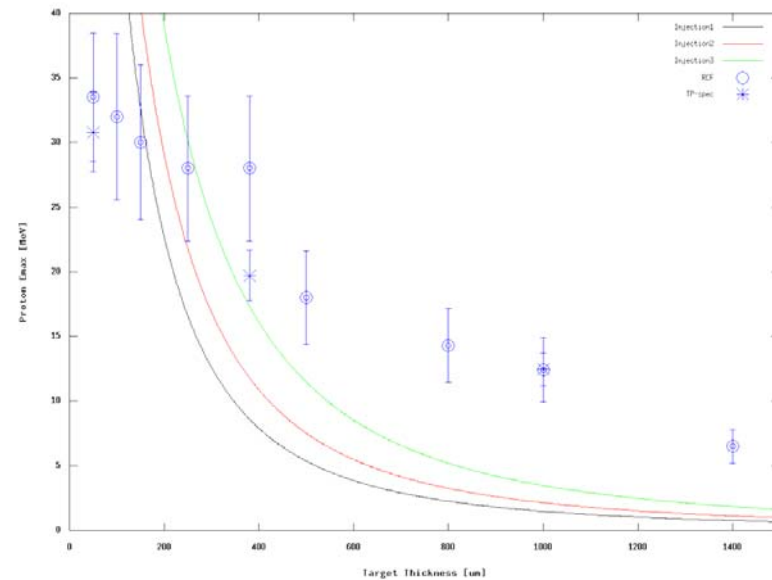
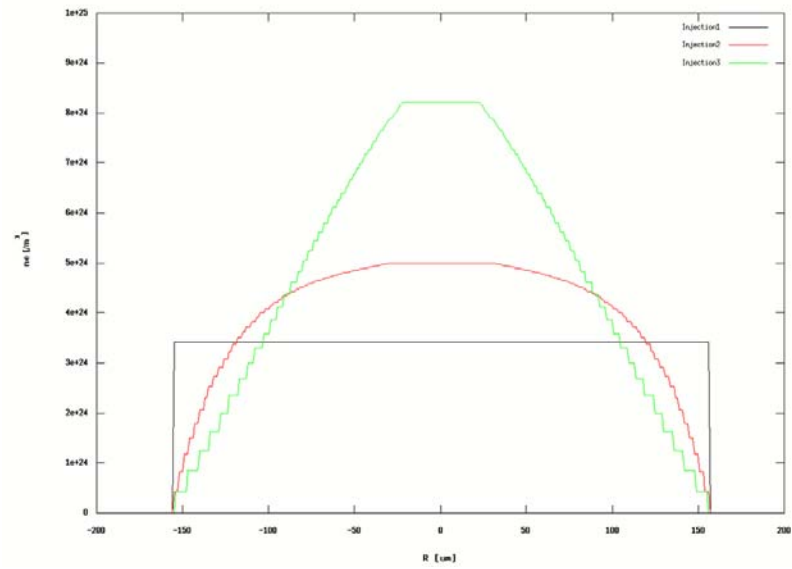
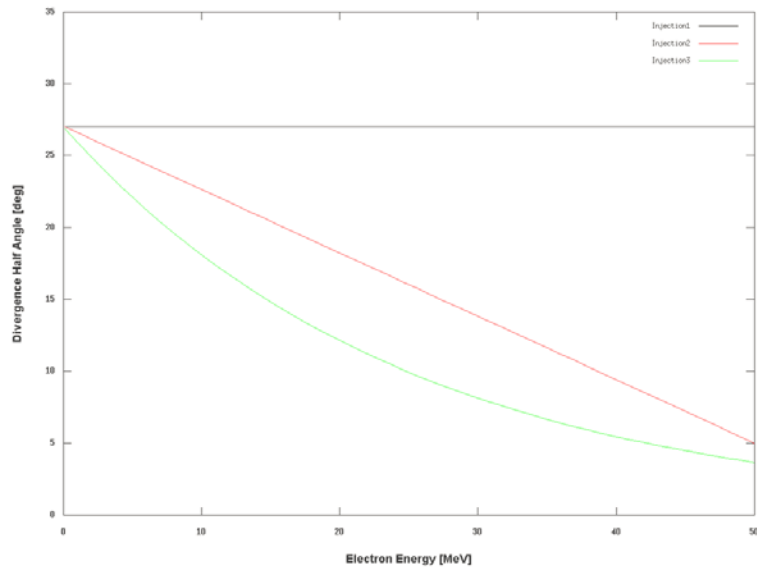


2 – Innovative nuclear diagnostics

Examples may include:

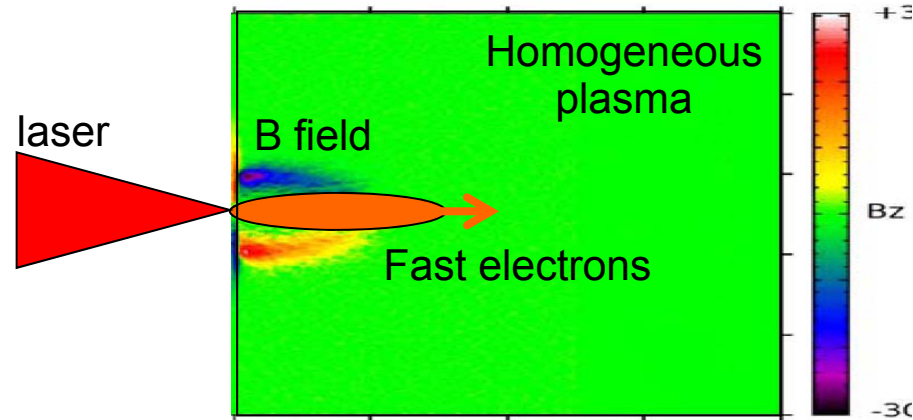
- fusion reaction history measurements using gamma detectors (NIF) ($\text{D} + \text{T} \rightarrow \gamma + ^3\text{He}$);
- charged particle detection to measure yield of neutronless reactions (e.g. $\text{D} + ^3\text{He} \rightarrow \text{p} (15 \text{ MeV}) + ^4\text{He}$);
- Higher nuclear yields expected; observation of lower cross section and higher threshold energy reactions;

Effect of angle change with energy



Magnetic collimation

Resistive generation of toroidal B-field. B-field pinches the fast electron beam



Magnetic field generation during electron propagation is described by combining Ohm's law with Faraday's law:

$$\frac{\partial \mathbf{B}}{\partial t} = -\nabla \times \mathbf{E}$$

Ohm's law $\mathbf{E} = -\eta \mathbf{j}_f$

η = resistivity

\mathbf{j}_f = fast electron current density

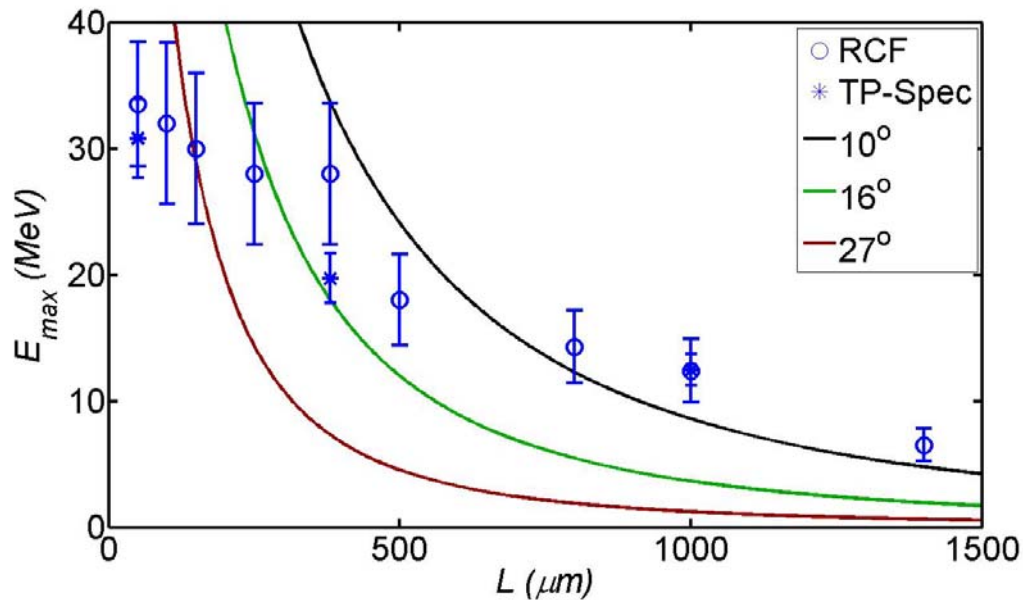
$$\frac{\partial \mathbf{B}}{\partial t} = \eta \nabla \times \mathbf{j}_f + (\nabla \eta) \times \mathbf{j}_f$$

Robinson and Sherlock, Phys. Plasmas, 14, 083105 (2007)

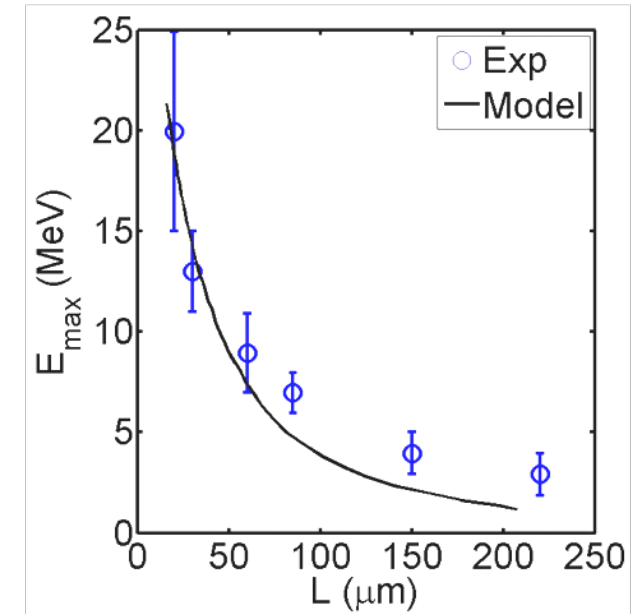
Generates a magnetic field that pushes electrons towards regions of higher current density

Generates a magnetic field that pushes electrons towards regions of higher resistivity

Results: Maximum proton energy



Yuan et al., Vulcan TAP



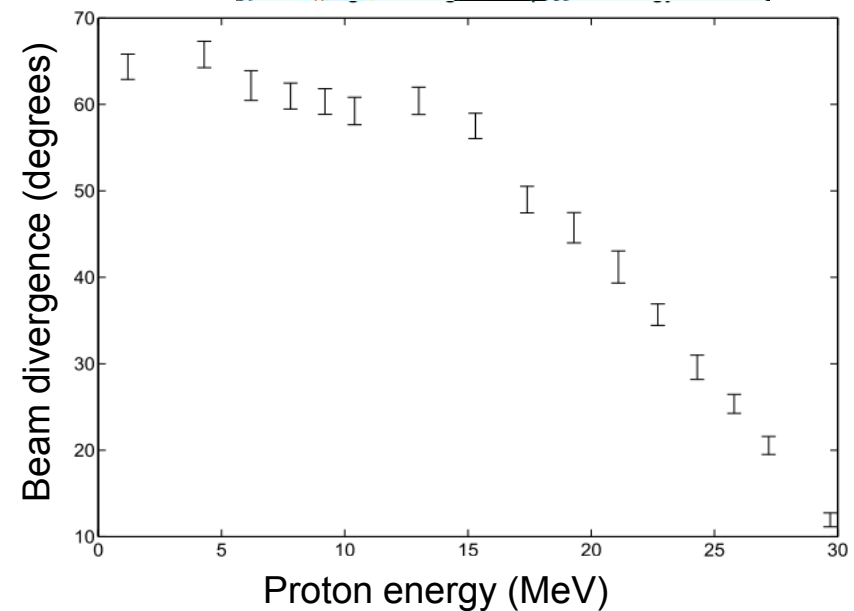
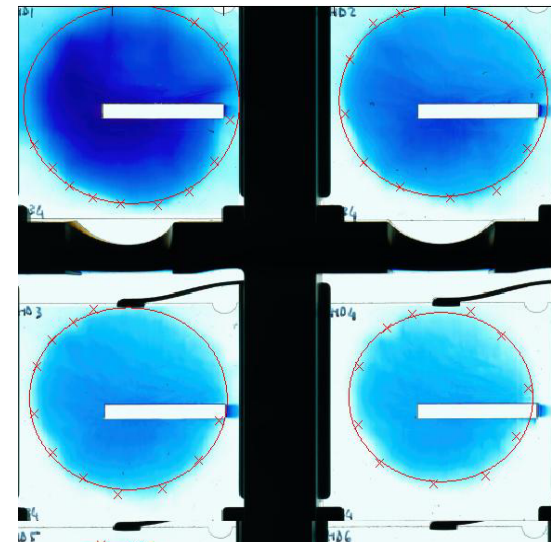
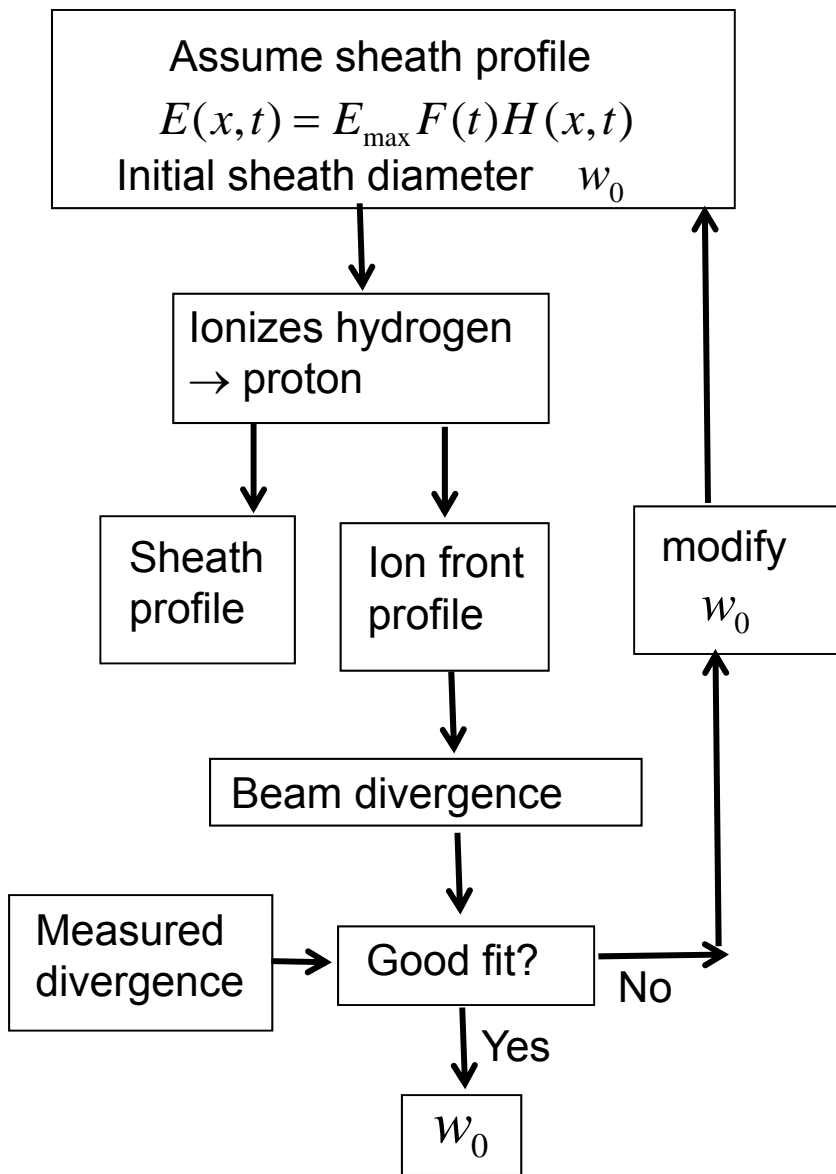
Fuchs et al., LULI (Nat. Phys. 2006)

Ballistic transport and P. Mora PRL 2003 plasma expansion model.

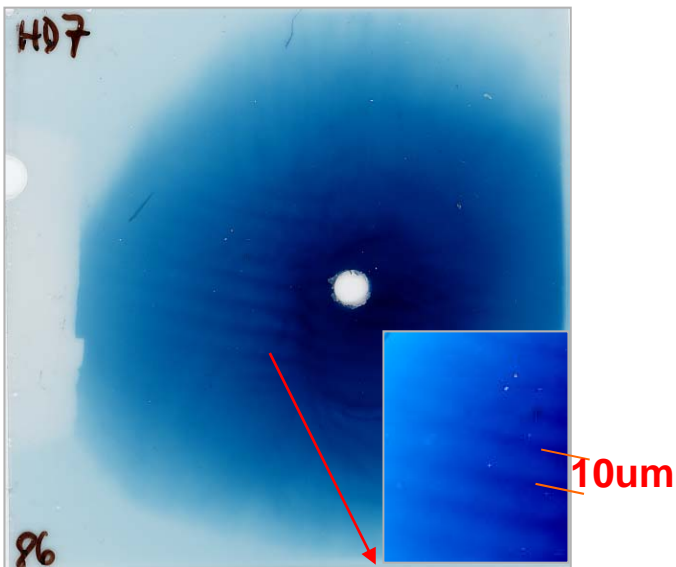
$$E_p \approx 2k_B T [\ln(\tau + \sqrt{\tau^2 + 1})]^2, \quad \tau = t_i \omega_{pp} / \sqrt{2e_N}, \quad \omega_{pp} \sim \sqrt{n_e} \sim 1/\phi_{sheath}$$

The scaling with target thickness is significantly different than expected from ballistic electron transport

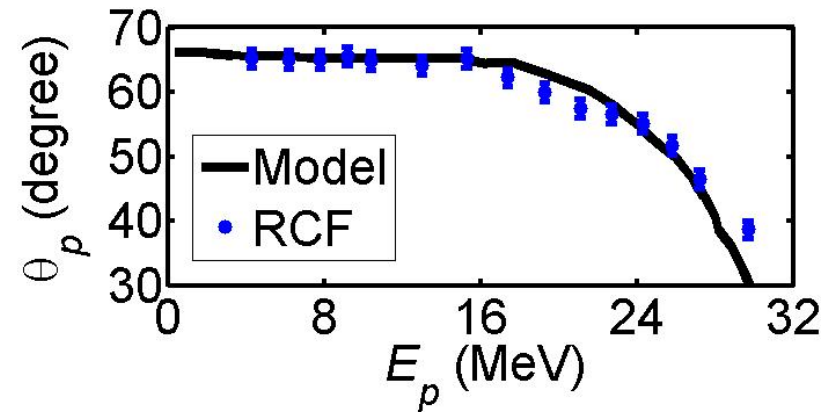
Sheath expansion is modelled



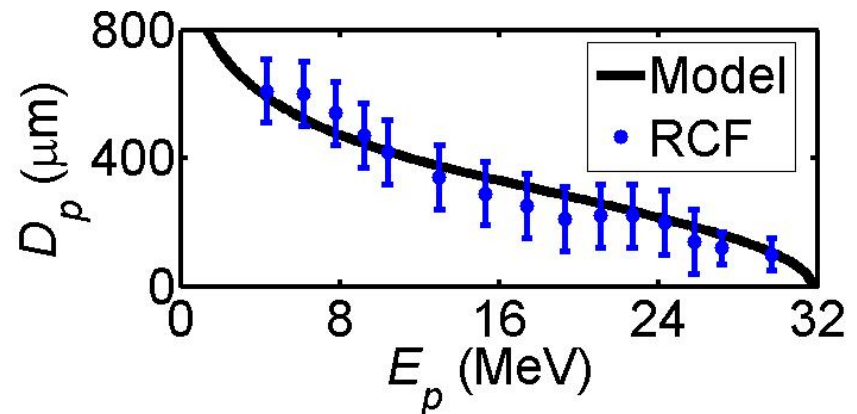
Model is benchmarked using grooved target results



Divergence



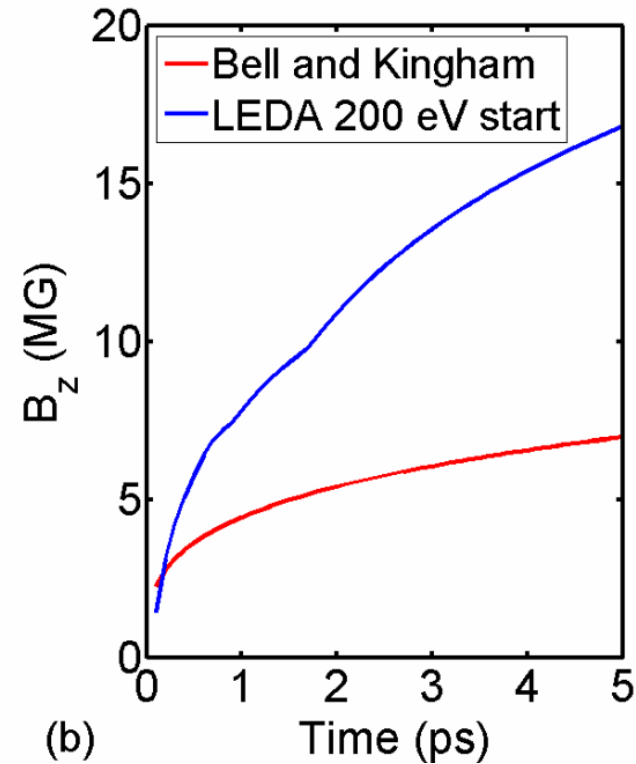
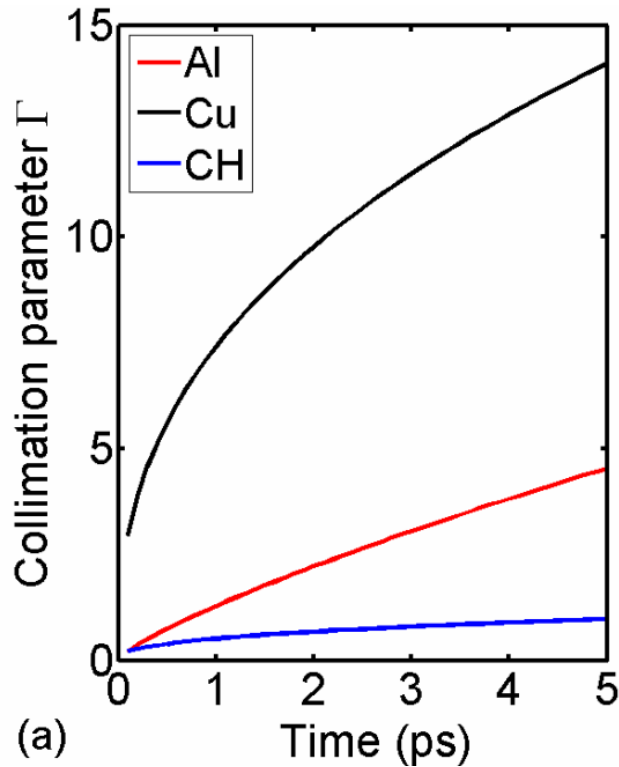
Source size



Scaling of the collimation effect

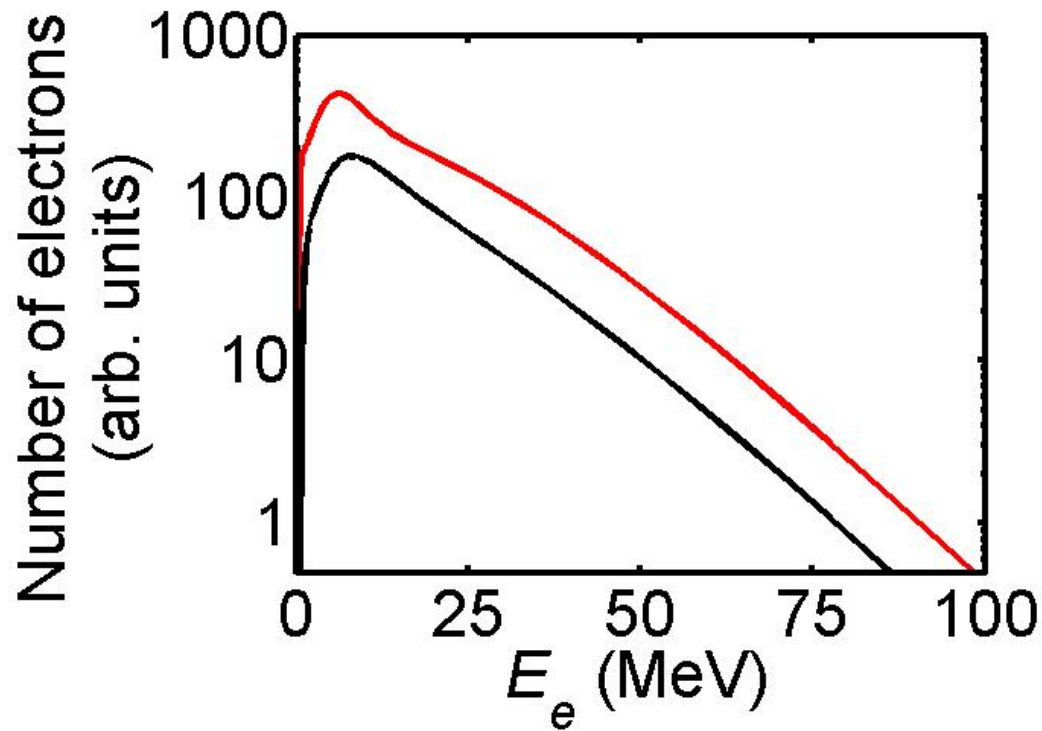
Bell-Kingham theory: In the limit of substantial heating, collimation parameter:

$$\Gamma = 0.13 n_{23}^{3/5} Z^{2/5} \ln \Lambda^{2/5} P_{TW}^{-1/5} T_{f,511}^{-3/10} (2 + T_{f,511})^{-1/2} R_{\mu m}^{2/5} t_{psec}^{2/5} \theta_{1/2,rad}^{-2}$$

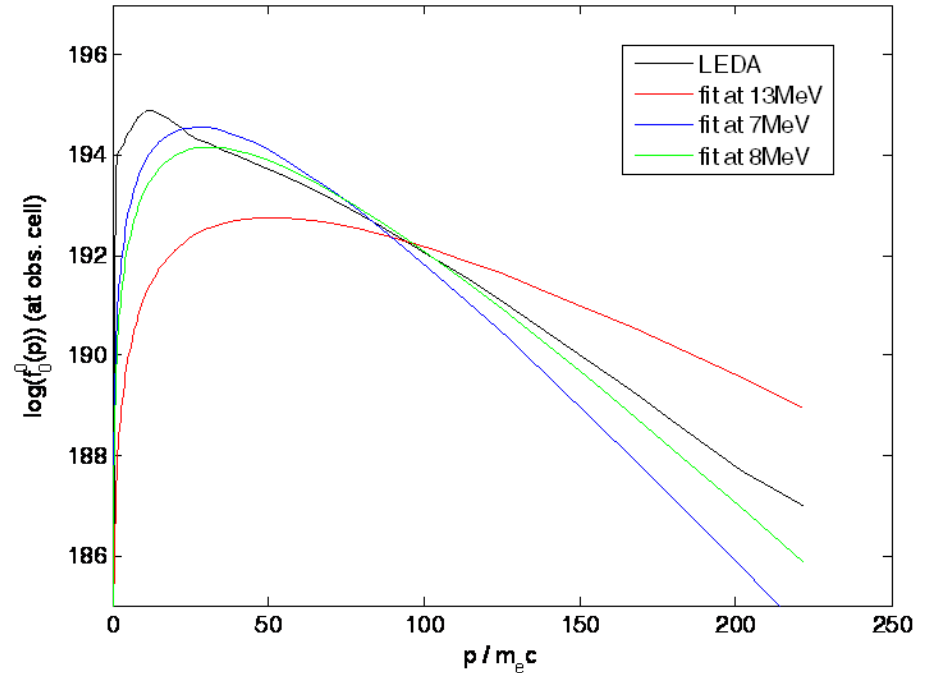
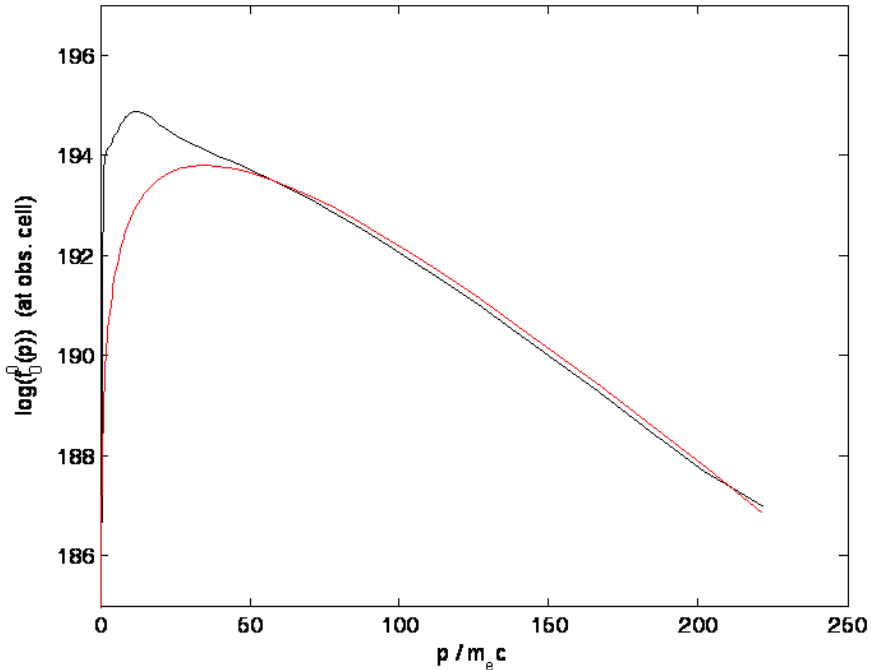




Electron temperature from LEDA simulations



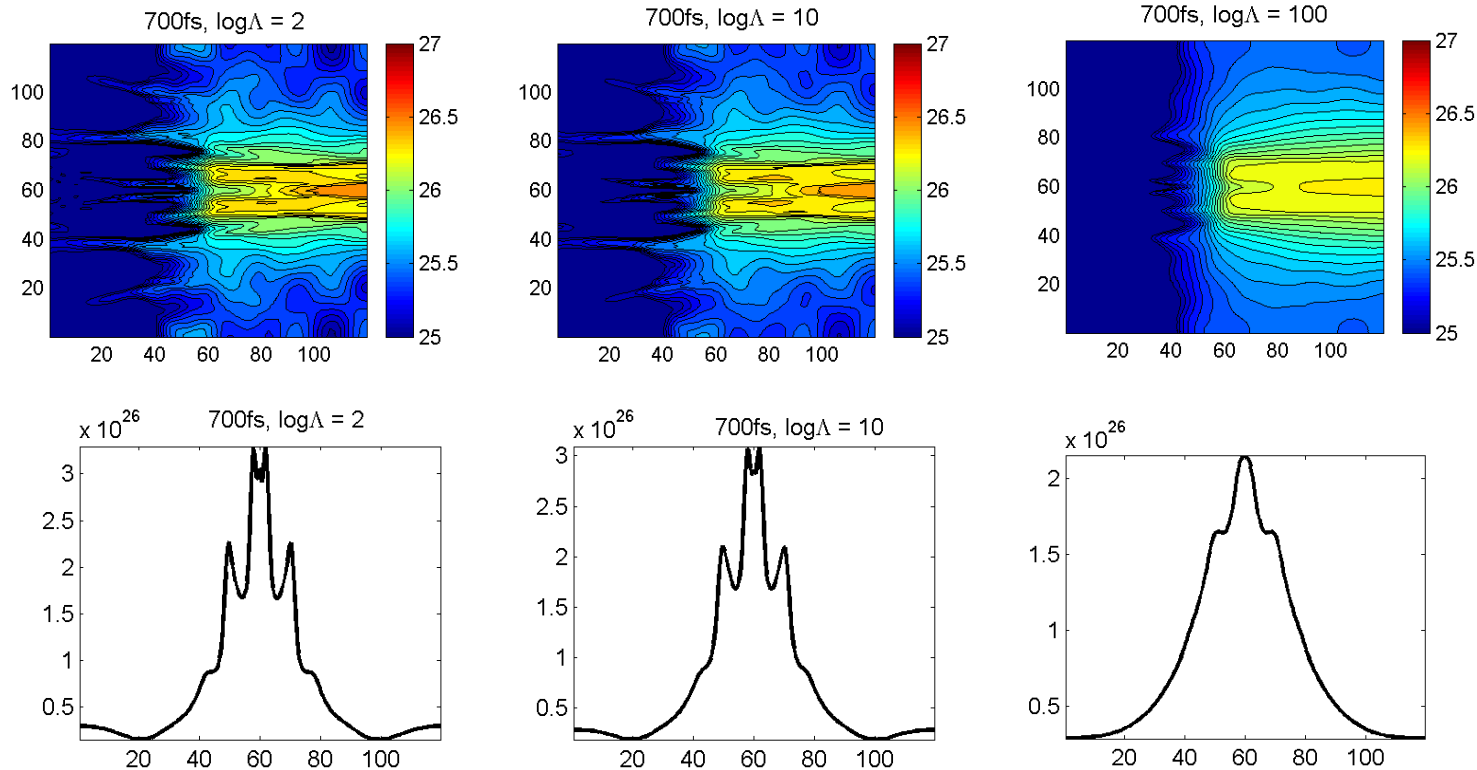
Temperature variation



Black line is electron spectrum at rear surface of a 400 micron Al target

Red is fit using the input electron distribution and temperature (9.2 MeV)
Same temperature!

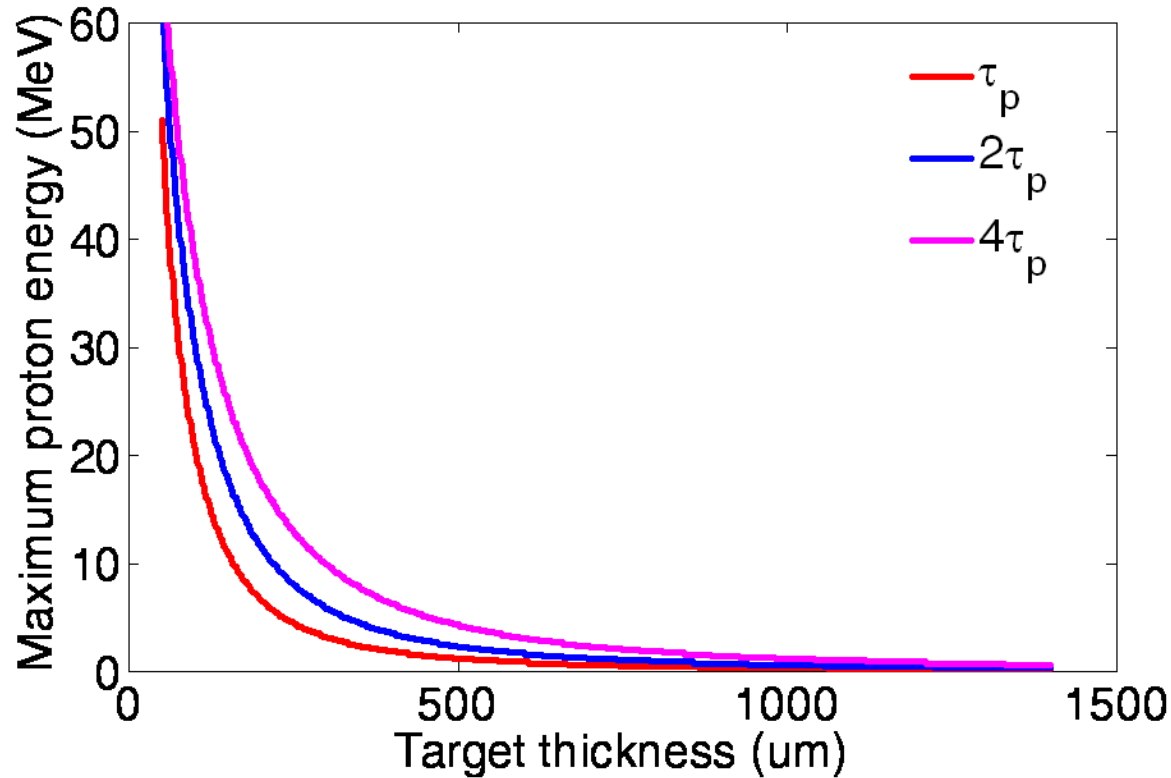
Artificially increasing scattering



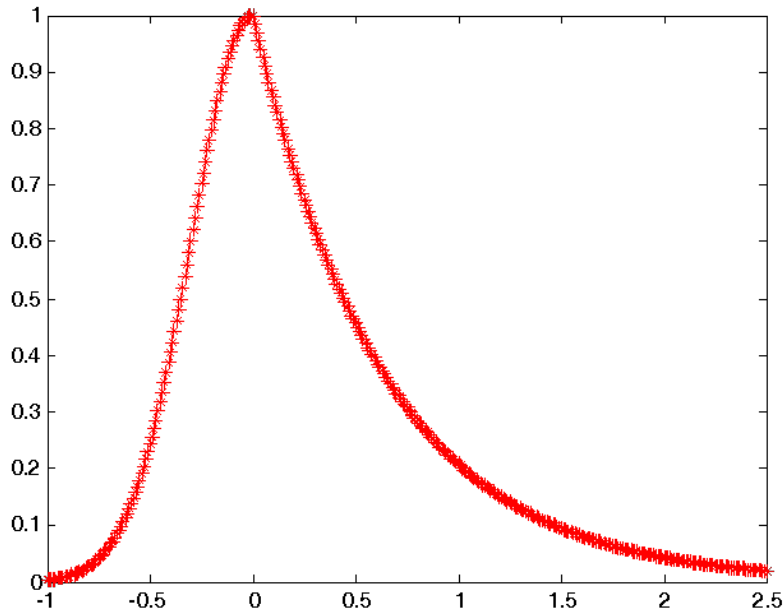
- Increase electron-ion scattering rate
 - $\log\Lambda = 2 \rightarrow 10 \rightarrow 100$
- Marginal effect on beam smoothness



Field duration variation



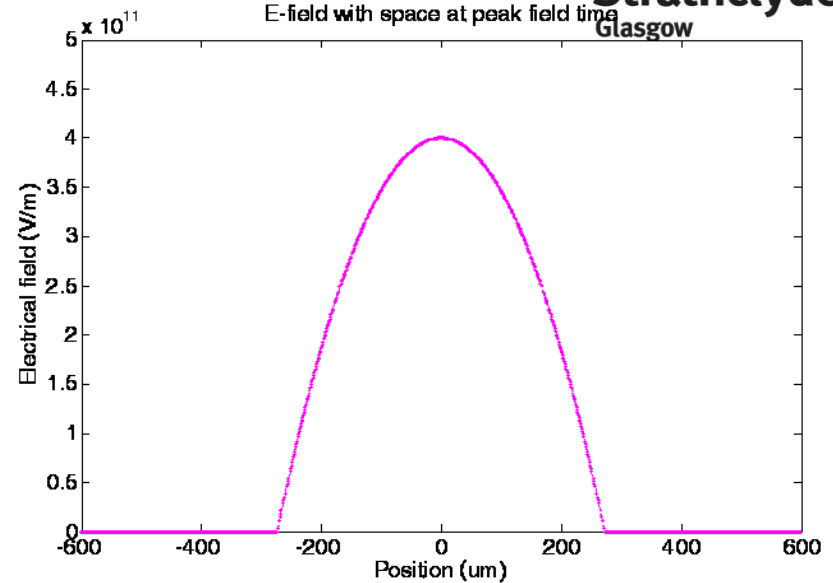
P Mora PRL 2003 plasma expansion model



The temporal evolution is assumed to be a combination of Gaussian increase and exponential decrease.

This trend is supported by LEDA simulation, as well as the previous reports.

McKenna et al PRL 98, 145001 (2007)
Kar et al PRL 100, 105004 (2008)



Electrical field transverse distribution is assumed to be parabolic function

$$E(x,t) = E_p F(t) H(x,t)$$

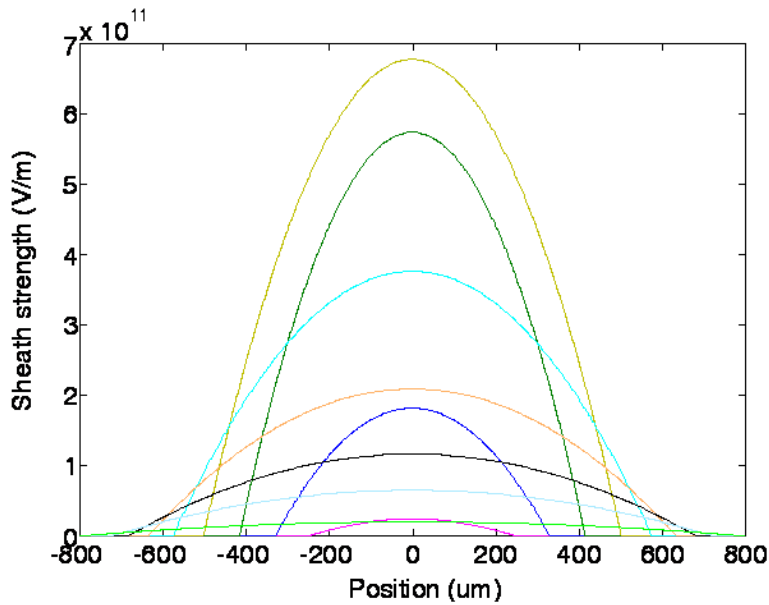
$$F(t) = \exp(-t^2 / 2\sigma^2) \quad t \leq 0$$

$$= \exp(-t/t_0) \quad t > 0$$

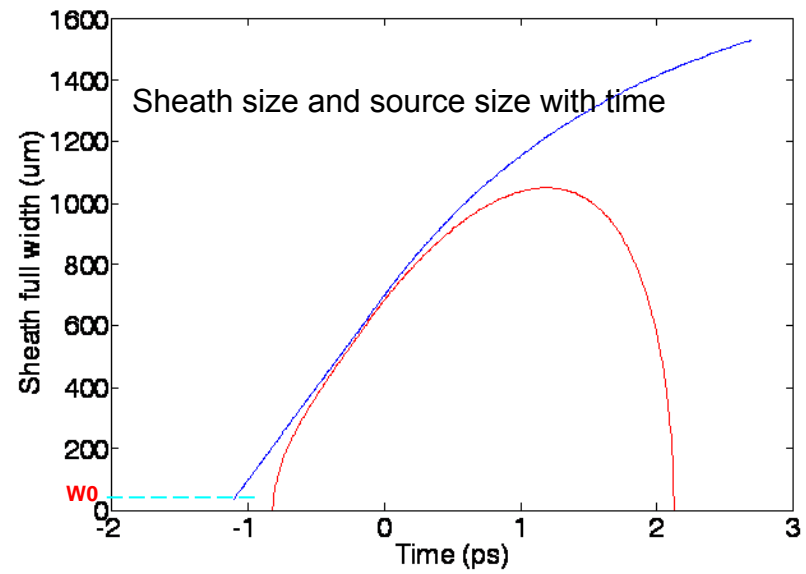
$$H(x,t) = 1 - x^2 / 4p(t)$$

$$p(t) = (w_0 + vt)^2 / 2$$

Carroll et al PRE 76, 065401 (2007)
Brambrink et al PRL 96, 154801 (2006)

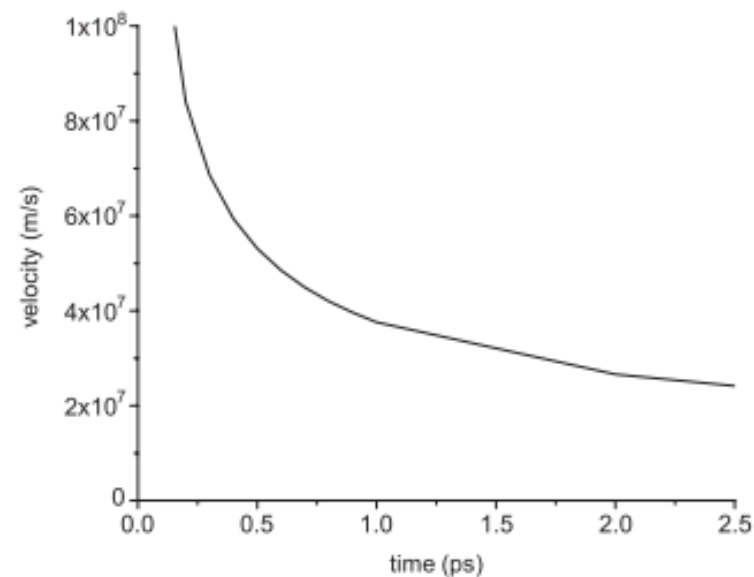
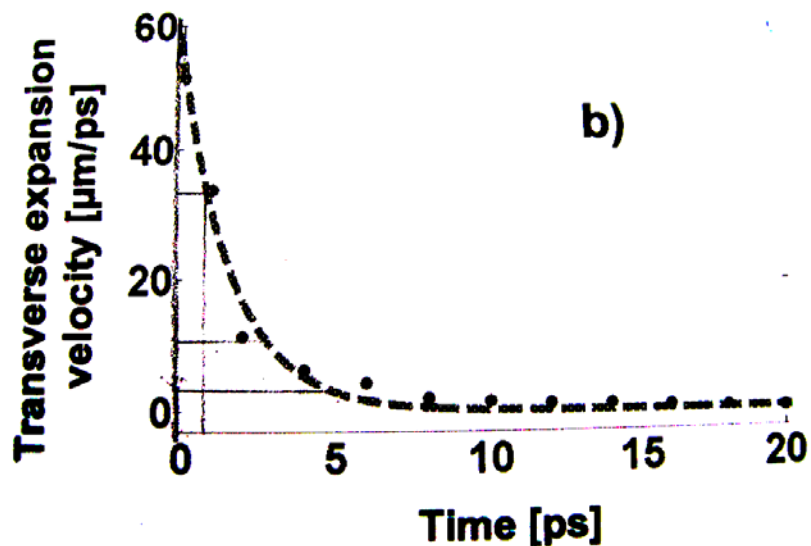


Example sheath field profiles at different time



An example fit of beam divergence

Transverse expansion velocity with time

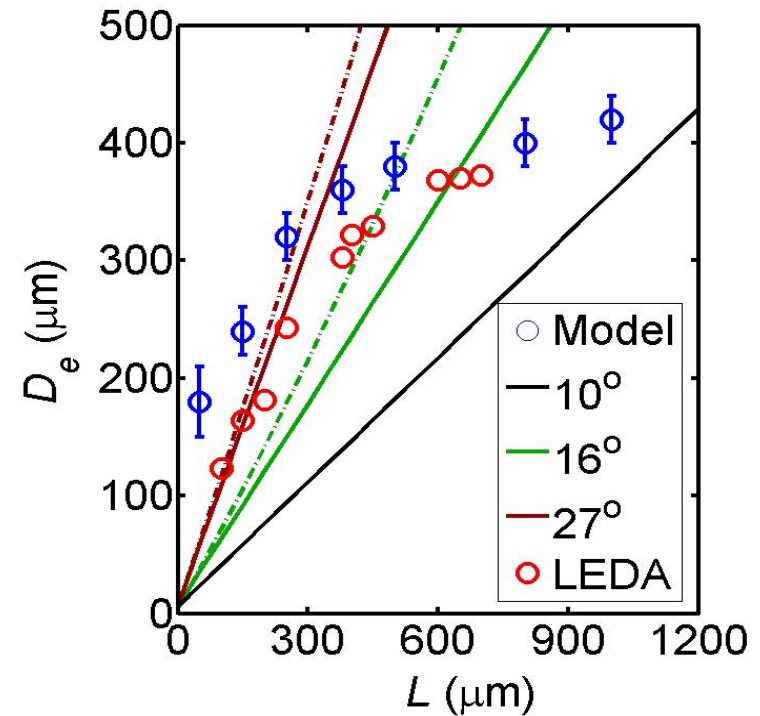
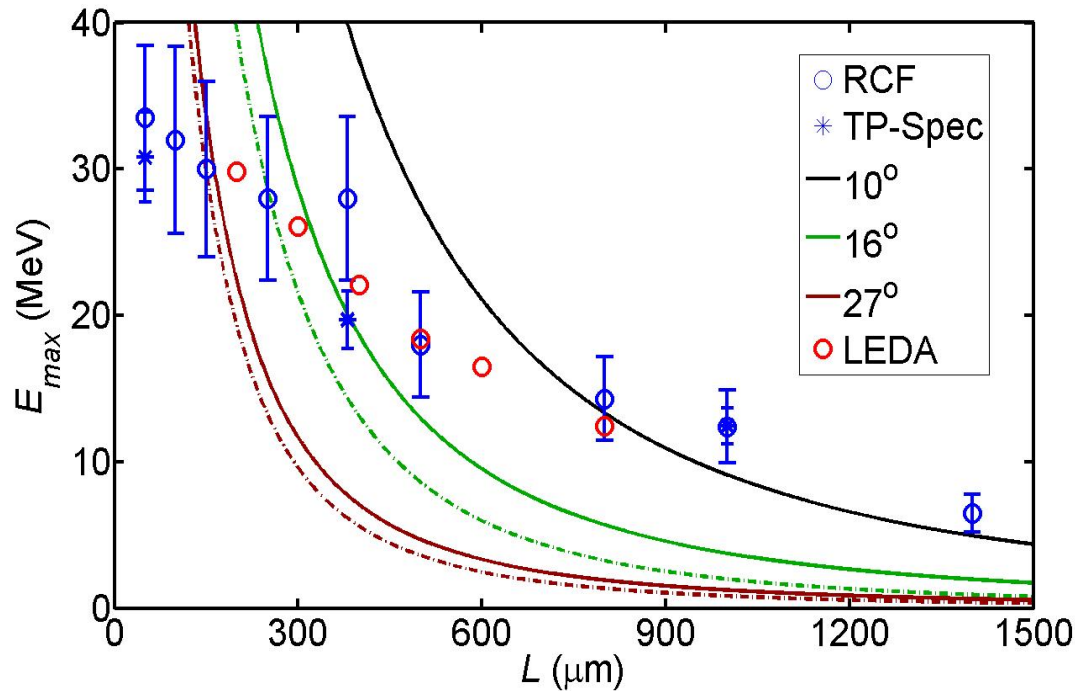


From Patrizio Antici's PhD thesis

E Brambrink et al PRL 96, 154801 (2006)

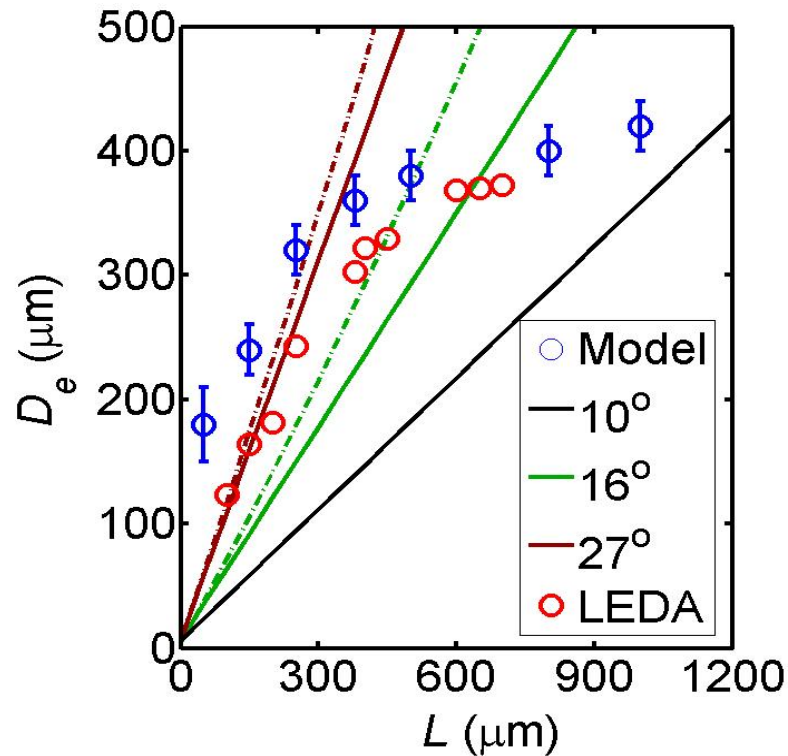
Both suggest an exponential decrease of expansion velocity with time

Comparing simulation and experiment results



Simulation densities used in plasma expansion model

Sheath size as a function of target thickness

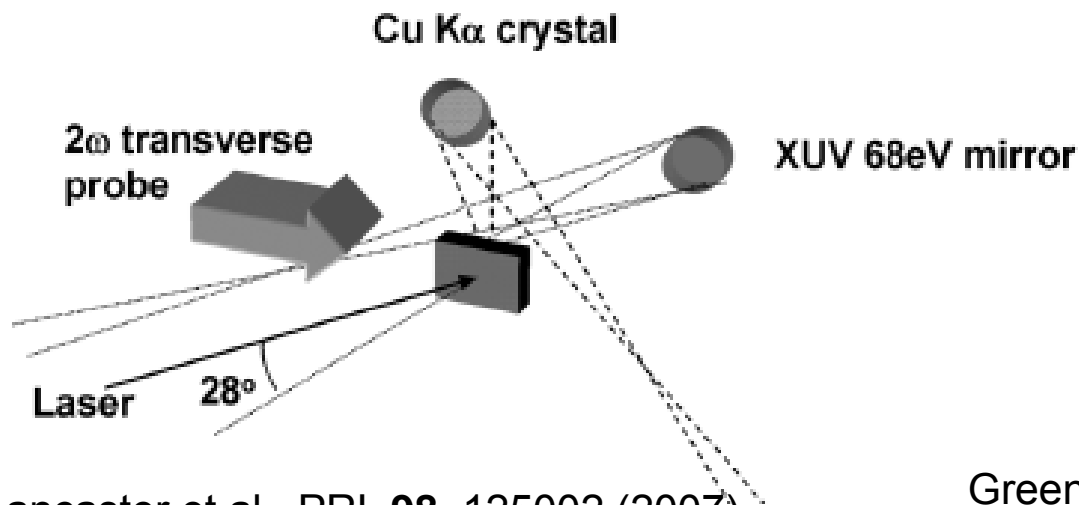


Reduced growth in sheath size for thick targets

Lateral expansion of the fast electrons is limited

Self-induced fields become more important in thicker targets

title

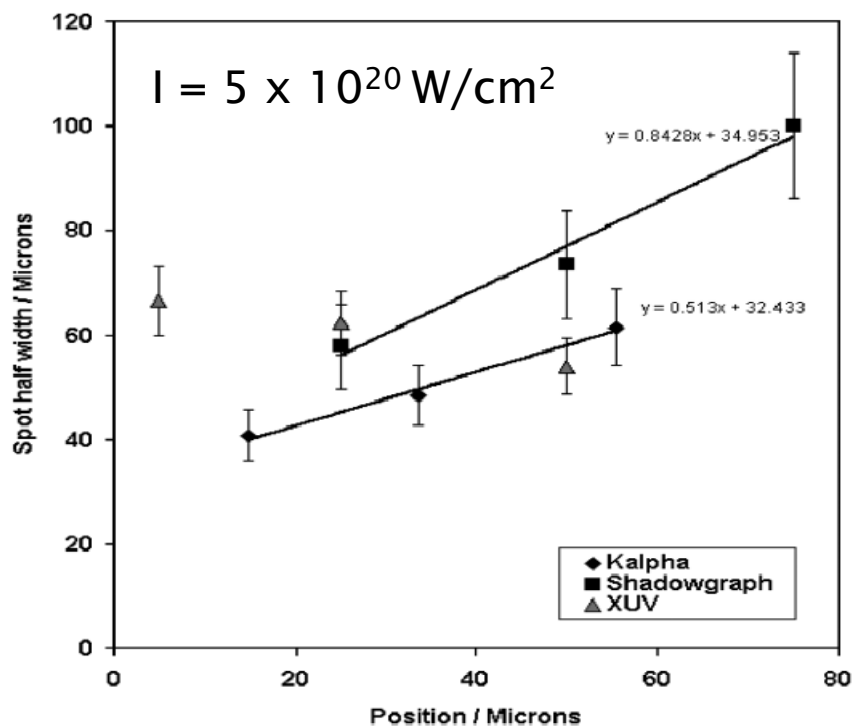


Target thicknesses $\sim 100 \mu\text{m}$

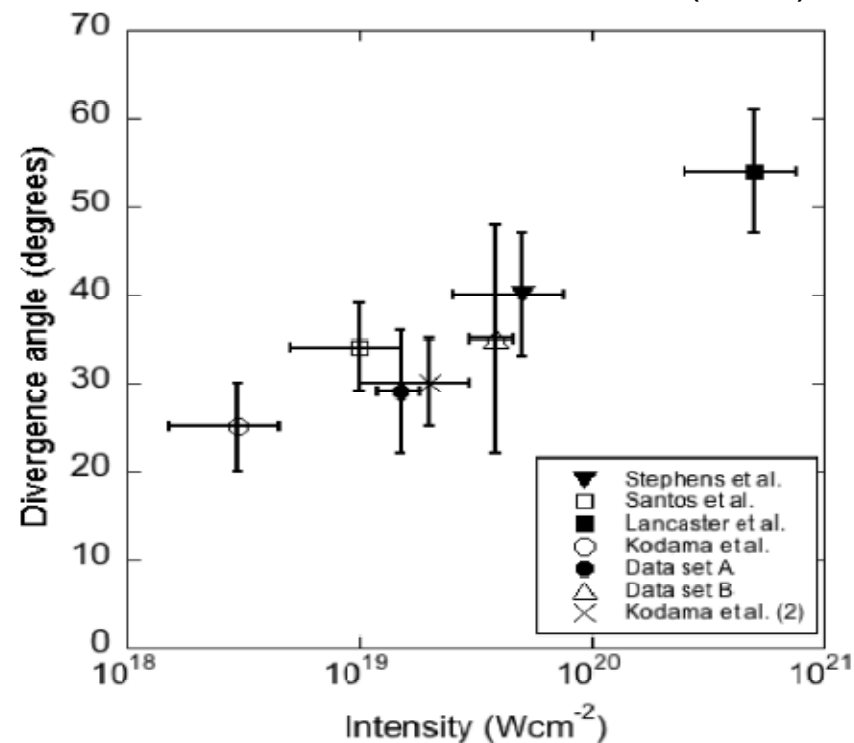
Diagnostics:

- K α emission
- XUV emission
- Shadowgraphy

Lancaster et al., PRL **98**, 125002 (2007)

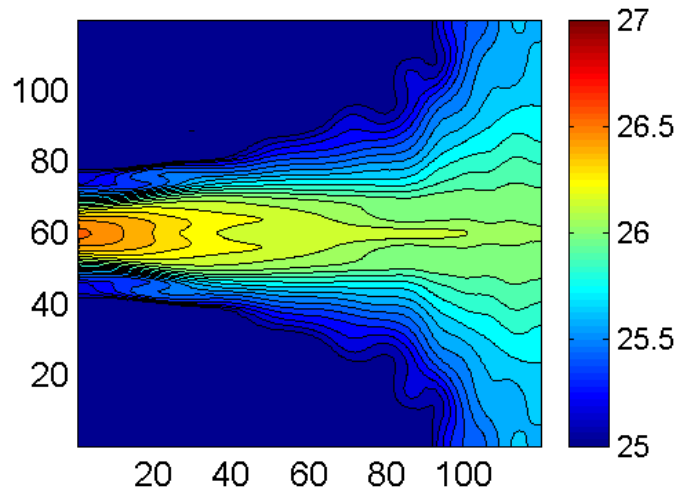


Green et al., PRL **100**, 015003 (2008)

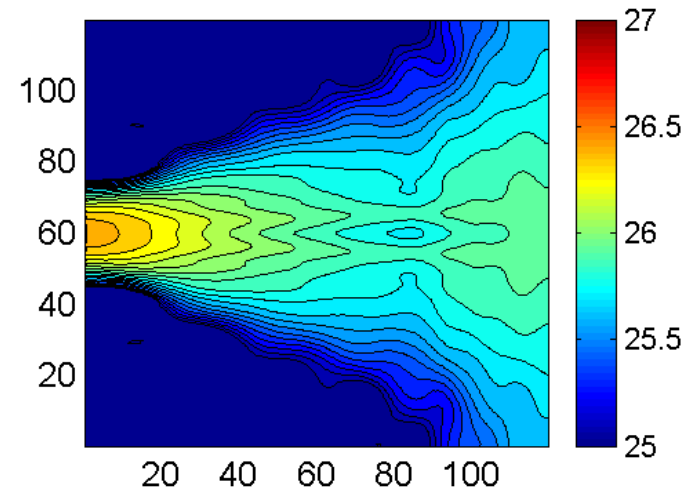


title

AL SIMULATION

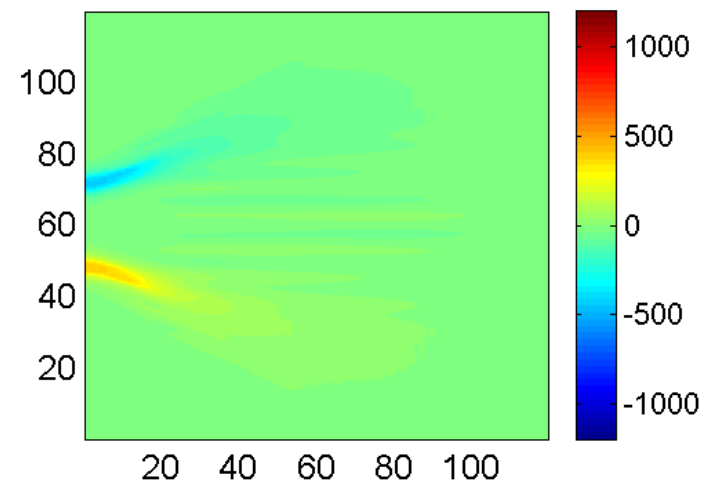
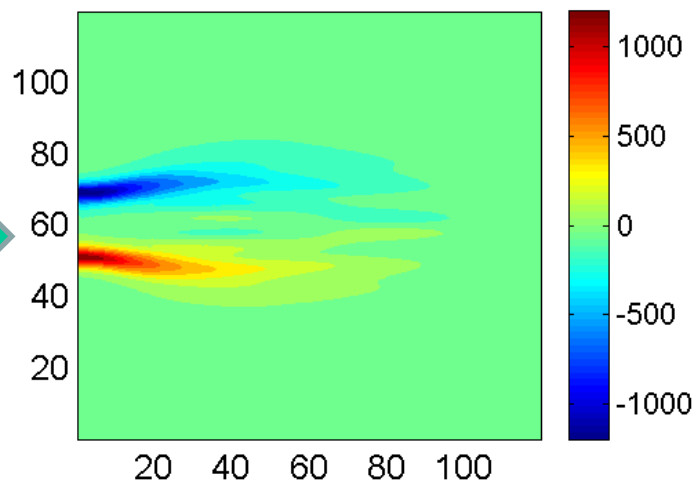


CH SIMULATION



Magnetic Fields

$y / \mu\text{m}$



$x / \mu\text{m}$